Phase transitions and phase diagram of the ferroelectric perovskite $(Na_{0.5}Bi_{0.5})_{1-x}Ba_xTiO_3$ by anelastic and dielectric measurements

F. Cordero,[1] F. Craciun,[1] F. Trequattrini,[2] E. Mercadelli,[3] and C. Galassi[3]

[1]*CNR-ISC, Istituto dei Sistemi Complessi, Area della Ricerca di Roma-Tor Vergata, Via del Fosso del Cavaliere 100, I-00133 Roma, Italy*
[2]*Dipartimento di Fisica, Università di Roma "La Sapienza", P.le A. Moro 2, I-00185 Roma, Italy*
[3]*CNR-ISTEC, Istituto di Scienza e Tecnologia dei Materiali Ceramici, Via Granarolo 64, I-48018 Faenza, Italy*

The complex elastic compliance and dielectric susceptibility of $(Na_{0.5}Bi_{0.5})_{1-x}Ba_xTiO_3$ (NBT-BT) have been measured in the composition range between pure NBT and the morphotropic phase boundary included, $0 \leq x \leq 0.08$. The compliance of NBT presents sharp peaks at the rhombohedral/tetragonal and tetragonal/cubic transitions, allowing the determination of the tetragonal region of the phase diagram, up to now impossible due to the strong lattice disorder and small distortions and polarizations involved. In spite of ample evidence of disorder and structural heterogeneity, the R-T transition remains sharp up to $x=0.06$, whereas the T-C transition merges into the diffuse and relaxorlike transition associated with broad maxima of the dielectric and elastic susceptibilities. An attempt is made at relating the different features in the anelastic and dielectric curves to different modes of octahedral rotations and polar cation shifts. The possibility is also considered that the cation displacements locally have monoclinic symmetry, as for PZT near the morphotropic phase boundary.

I. INTRODUCTION

The phase diagrams of the solid solutions of the ferroelectric perovskite $Na_{0.5}Bi_{0.5}TiO_3$ (NBT) with other tetrahedral perovskites are actively studied, mainly with the intent of obtaining compositions close to a morphotropic phase boundary (MPB) between rhombohedral (R) and tetragonal (T) phases, with easily reorientable ferroelectric domains and high electromechanical coupling. In fact, NBT based perovskites are among the possible lead-free piezoelectric materials that would substitute the widely used $PbZr_{1-x}Ti_xO_3$, when new environmental legislations will limit the use of Pb containing materials.

The phase diagram of $(Na_{0.5}Bi_{0.5})_{1-x}Ba_xTiO_3$ (here abbreviated as NBT-BT or BNBT-100x) is still uncertain in the interesting region $x < 0.1$ including the MPB, particularly regarding the nature and extension of the presumably almost antiferroelectric (AFE) phase that becomes ferroelectric (FE) on further cooling. Also the temperature evolution of the structure of undoped NBT is the object of contradictory interpretations.[1] The main difficulties in determining the structure of NBT by neutron or x-ray diffraction are due to the very low distortion in both the tetragonal and rhombohedral phases, with a cell distortion from cubic of $<0.2\%$ and $\sim 0.4\%$, respectively,[2] and to the structural disorder in the Na/Bi sublattice, which is averaged out and compensated by anomalously large thermal factors in the analysis.[3] In addition, x-ray diffraction is little sensitive to the rotations of the O octahedra involved in the various structural transformations, due to the low atomic number of O. Cation disorder is enhanced in the solid solutions with other perovskites; it is responsible for the diffuse nature of the lower temperature transitions in the dielectric measurements, sometimes considered of the relaxor type, and possibly for the very broad temperature range of coexistence between T and R phases, with characteristics that vary from study to study. There is also scarce reproducibility of the transition temperatures and

of the associated anomalies in the dielectric and other physical properties, which generally exhibit very broad anomalies with large hysteresis between heating and cooling.[1,4] These uncertainties may also be connected with differences from sample to sample in the local cation ordering and nonperfect stoichiometry in the Na/Bi sublattice, due to preferential loss of Bi during sintering.

The elastic constants should provide clear information on the occurrence of transformations between C, T, and R phases, which are of ferroelastic nature, but only few studies of the acoustic properties of NBT exist,[4–6] which have not an obvious connection with the known phase transitions. Here we present an extensive study of $(NBT)_{1-x}(BT)_x$ with $0 \leq x \leq 0.08$ by combined anelastic and dielectric spectroscopies.

II. EXPERIMENTAL

Powders of the composition $(Na_{0.5}Bi_{0.5})_{1-x}Ba_xTiO_3$ with $x=0$ and $x=2, 3, 4, 5, 6, 8$ mol % were prepared following the mixed-oxide method. Stoichiometric amounts of Na_2CO_3 (Merck 6392), Bi_2O_3 (Aldrich 223891), $BaCO_3$ (Merck 1714), TiO_2 (Degussa P 25) were mixed in ethanol with zirconia milling media for 48 h, dried and sieved. For each composition the calcining and sintering temperatures were systematically investigated in order to improve the cold consolidation behavior and the final density. After heat treatment at $700–800 \degree C$ for 1 h and further milling and drying, the powders were isostatically pressed at 300 MPa and sintered at $1150 \degree C$ for 2 h. In order to avoid the loss of Na and Bi, which is significant at temperatures over $1000 \degree C$, most of the sintering processes were carried out with the samples placed on a ZrO_2 disk, covered with an Al_2O_3 crucible and sealed with NBT pack. The x-ray diffraction analysis evidenced the pure perovskitic phase in all the samples investigated. The microstructure of the sintered samples was observed on polished and etched surfaces by means of scanning electron microscopy (Leica Cambridge Stereoscan 360). De-

pending on the composition (at the same sintering conditions) the microstructures result more or less homogeneous, with some large, squared grains in a matrix of smaller grains; among those sintered in the NBT pack powder, pure NBT showed the largest grain size (5–20 μm), which reduced upon addition of barium, the lowest mean size being found with $x = 0.08$ (0.5 μm).

We prepared disks (diameter 22 mm, thickness 2 mm) for the dielectric measurements and blocks ($60 \times 7 \times 7$ mm^3) subsequently cut into bars ($40 \times 4 \times 0.6$ mm^3) for both anelastic and dielectric experiments. The faces of the disks were ground, silver electroded and poled with an electric field of 3 kV/mm in a silicon oil bath at 120 °C for 30 min, while the bars were tested unpoled.

The dielectric measurements were carried out on poled and unpoled disks and bars in a frequency range between 200 Hz and 200 kHz using a Hewlett-Packard LCR meter (HP 4284A) with a four wire probe and an ac driving signal level of 0.5 V/mm. The dielectric permittivity $\varepsilon = \varepsilon' - i\varepsilon''$ was obtained from the measured values of capacitance and loss $\tan \delta = \varepsilon''/\varepsilon'$. The measurements were made on heating/cooling at 1–1.5 K/min between 300 and 570 K in a Delta Design climatic chamber model 9023A.

The complex Young's modulus $E = E' + iE''$ was measured by electrostatically exciting the flexural vibrations of the bars, which were suspended on thin thermocouple wires in vacuum. It was possible to excite the first, third, and sometimes fifth flexural modes, whose resonating frequencies are in the ratios 1:5.4:13. The fundamental frequency is given by[7]

$$f = 1.028 \frac{h}{l^2} \sqrt{\frac{E}{\rho}},$$

where l is the length, h the thickness, ρ the density the bar; for most samples it was $f \sim 1.4$ kHz. From the above formula it is possible to extract the absolute value of the Young's modulus. Such a value is affected by an error that may easily be of the order of 10%, due to uncertainties in the sample dimensions, porosity (the density was always 93.7–98.6 % of the theoretical one) and above all due to the Ag electrode, which was applied to one or two faces and whose thickness and Young's modulus could not be controlled. The anelastic spectra are displayed in terms of the real part of the reciprocal Young's modulus or compliance, $s = E^{-1} = s' - is''$, and of the elastic energy loss coefficient $Q^{-1} = s''/s'$. Since the anelastic spectroscopy experiments were made in vacuum, some oxygen loss occurred when 800 K was exceeded, and the sample became darker. In most cases, however, we did not note any effect on the anelastic and even dielectric spectra; major changes occurred if 1000 K was exceeded with samples prepared without precautions against Bi loss during sintering.

III. RESULTS AND DISCUSSION

A. Undoped NBT

1. Anelastic spectrum of NBT

Figure 1 shows the compliance curves $s'(T)$ and the losses $Q^{-1}(T)$ of undoped NBT measured on heating and
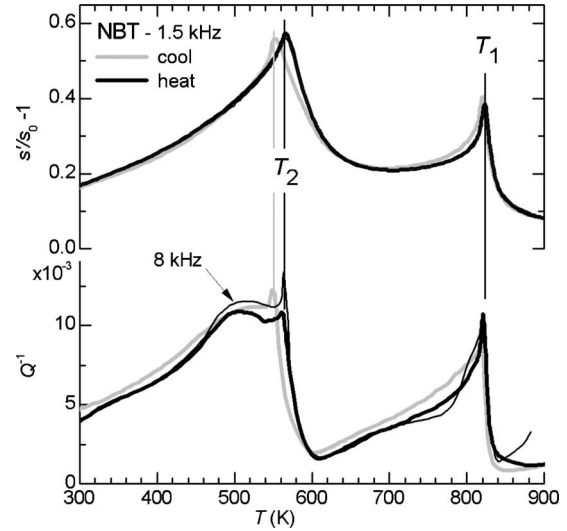

FIG. 1. Reciprocal Young's modulus $s' = 1/E'$ and elastic energy loss Q^{-1} of NBT measured during heating (black) and cooling (gray) at 1.4 kHz (thick lines) and 7.4 kHz (thin line, only heating).

cooling at 1.5 kHz (thick black and gray lines); the thin black curves were measured at 8 kHz during heating and are practically coincident with those at 1.5 kHz, especially in the real part. This means that the anomalies in s' are not due to relaxation of domain walls or defects, but they reflect the intrinsic elastic constants plus the fast relaxation of the order parameters involved in the structural transformations, which can instantaneously follow the sample vibration. Some frequency dependence is observed in the losses, and may be due to the relaxation of domain walls. There are sharp peaks at $T_1 = 823$ K and $T_2 = 564$ K (during heating) in the complex compliance, whose sharpness is in contrast with the broad anomalies in the other physical properties, including the acoustic ones in the gigahertz range, and with the structural changes, which are faint and spread over wide temperature ranges. The anomalies appear at slightly lower temperature during cooling, with hystereses of 3 and 13 K for T_1 and T_2, respectively.

2. Phase transitions in NBT

The picture of the structural transformations in pure NBT is still confused and contradictory; therefore, in order to relate the elastic anomalies of Fig. 1 to structural changes, we replotted our data in Fig. 2(a), together with the dielectric susceptibility and the temperature dependencies of various structural parameters measured in other experiments.

For clarity, the labels of the ordinates are omitted; only the temperature dependences are relevant here. Starting from the bottom panel (a), the curves s' and Q^{-1} measured during heating determine the temperatures T_1 and T_2. In the next panel (ordinates: $0 \leq \varepsilon' \leq 3000$) curve 1 is the dielectric permittivity ε' measured during heating on poled NBT at 10 kHz. The step at ~470 K occurs at the same temperature where the macroscopic polarization vanishes, and the $P-E$ hysteresis loops become narrow or pinched in the center, and which is therefore called depolarization temperature T_d; it defines the transition between FE and possibly AFE (Refs.
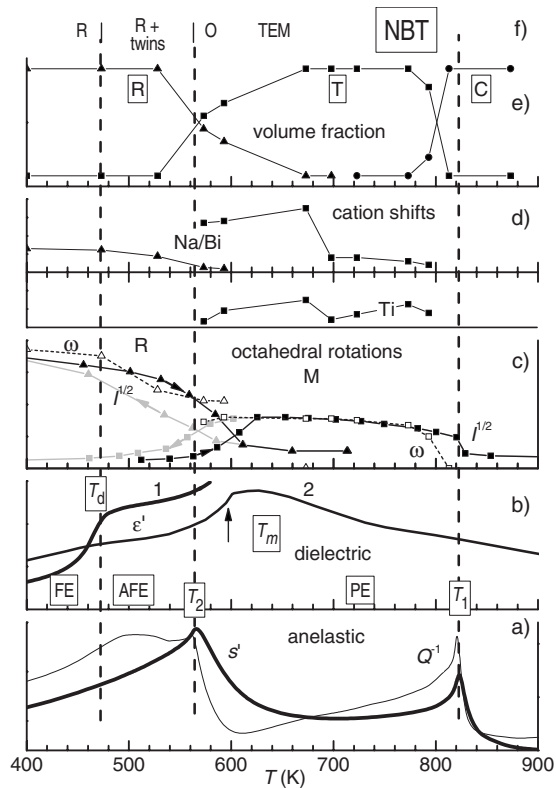
FIG. 2. Temperature dependence of various properties of NBT from our measurements and from the literature, as explained in the text.

8–10) state. The antiferroelectric nature of the phase at $T > T_d$ is not unanimously accepted[11–13] and is deduced, besides from the shape of the $P-E$ hysteresis curves, from the broad maximum of ε' around $T_m \sim 630$ K, which would signal the transition from AFE to paraelectric (PE). The width of this maximum, a possible slight frequency dispersion, especially at high frequencies,[14] the fact that no structural transformation at T_m but instead several indications of phase coexistence on nanoscale exist,[3,15,16] induce several authors to liken this diffuse transition to a relaxor transition not only in the solid solutions with BT or other ferroelectrics, but also in pure NBT.[3,4,17–20] The frequency dispersion is however definitely smaller than for traditional relaxors.[8,14] Due to limitations in the temperature range of our apparatus, we could neither reach the T-C transition nor the maximum of ε' at T_m, and therefore we report curve 2 from Ref. 9, with a reduced step at T_d and an additional step, indicated by an arrow, connected with the R-T transition at a temperature higher than our T_2. The position, amplitude and shape of such a step is highly variable from experiment to experiment,[8,21] while a dielectric anomaly has never been observed at T_1.

Figure 2(c) presents the temperature dependence of the rotations of the octahedra determined by neutron diffraction[2,11] (ordinates: $0 \le \omega \le 8°$). In the case of NBT, the tetragonal structure arises from rotations of the octahedra about their c axes ($a^0a^0c^+$ in Glazer's notation[22]), giving rise to superlattice peaks from the M point of the Brillouin zone, while the rhombohedral structure is due to rotations about all

three principal directions of the cubic cell, with alternate sign along each axis ($a^-a^-a^-$ in Glazer's notation), giving rise to R-type superlattice peaks. The closed symbols (black =heating and gray=cooling) are the square root of the intensities of these superlattice reflections,[11] which should be proportional to the squares of the angles ω of rotations of type M and R.[23] They are scaled in order to overlap with ω measured from Rietveld refinements[2] (open symbols). The curves from the two experiments[2,11] are in reasonable agreement with each other and represent the rotational order parameters of the two transitions. On cooling from the C phase, the M rotation (squares) has an onset at $T_1 \sim 820 \pm 5$ K, no hysteresis between heating and cooling and a precursor tail extending a hundred Kelvin above T_1, at least in the experiment of Vakhrushev *et al.*[11] This behavior is close to what expected for the condensation of a soft M phonon mode at the zone boundary, acting as order parameter of the T phase. The softening of such a mode has been deduced from the intensity of the quasielastic neutron scattering at the M point,[11] but not observed by other techniques. On further cooling, the R rotations (triangles) start being observed below ~610 K and the amplitude of the M rotations decreases. On the basis of these curves, the onset temperature for the R-T transformation cannot be defined with an uncertainty smaller than 40 K and there is a hysteresis of 60 K between heating and cooling. Again, a softening of the R phonon mode in the T phase has been deduced from the intensity of the quasielastic scattering at the R point.[11]

The cation shifts with respect to the octahedra deduced from the neutron Rietveld refinements[2] are plotted in Fig. 2(d). In the ferroelectric R phase both the Na/Bi and Ti (not shown) shifts are parallel to the pseudocubic [111] direction; in the T phase, they are parallel to the tetragonal axis but with opposite signs, so that the structure is only weakly polar, in agreement with the nearly antiferroelectric properties in this temperature region. It is not clear whether the jump in cation shifts near 680 K may be put in relation with the broad dielectric maximum at T_m. The refinements of the neutron scattering data of Jones and Thomas[2] indicate regions of coexistence of C and T phases below T_1 and R and T phases around T_2 [volume fractions in Fig. 2(e)]. Unfortunately, the large temperature intervals between successive measurements did not allow to clarify the controversy on the R-T coexistence regions, as discussed by the same authors.[2] A later diffuse neutron scattering study[13] indicates a non trivial transformation between R and T structures over an extremely broad range of temperatures with a residual modulation of the R phase along the c axis of the parent structure. A modulated R structure is found also in recent TEM experiments,[1,16] which are interpreted in terms of a low temperature $R3c$ structure, which above 473 K starts twinning parallel to the [010] pseudocubic planes. On further heating, the density of *Pnma* twin planes increases and the modulation of the polarization direction gives rise to antiferroelectric properties until at 563 K the modulation disappears and the structure becomes homogeneous, identified as *Pnma* orthorhombic rather than tetragonal.[16] The temperatures of appearance and disappearance of the striation in the TEM images are indicated as vertical bars in Fig. 2(e), and correspond to T_d and T_2.

3. Identification of the elastic anomalies

Based on Fig. 2 and the above discussion we can identify the temperatures T_1 and T_2 of the peaks in the elastic compliance with the onsets of the T-C and R-T transformations. The first case is obvious, in view of the coincidence of T_1 with the onset of the M-type rotations of the octahedra [Fig. 2(c)] causing the tetragonal distortion. The fact that the T-C transformation is evident in the elastic but absent in the dielectric susceptibility[8,9] confirms that it is triggered by the nonpolar rotational mode of the octahedra, as already discussed in connection with optical and high-frequency dielectric measurements.[14] The small hysteresis of 3 K between heating and cooling indicates that the transition is almost second order. According to the Landau theory of phase transitions without fluctuations, the expected effect on the elastic constants involved in the resulting tetragonal distortion is a negative step when passing from cubic to tetragonal at T_1,[24] or equivalently a positive step in the compliances. The elastic anomaly at T_1 has a consistent peaked component besides the step, but clearly corresponds to the almost second order T-C transition. The occurrence of the additional peaked softening is common in perovskites and is usually explained in terms of fluctuation effects;[24] it will not be discussed further here.

The R-T transition is characterized by a variety of apparently contradictory experimental results, which generally agree on the diffuseness of the transition and broad range of coexistence of the two phases; the competition between the two M and R rotational instabilities even suggests the possibility of glassy behavior.[13] In some dielectric measurements there is a step near the region of R-T coexistence, but only on heating and not on cooling[8,25] and with varying temperatures and shapes.[9,25,26] The dielectric permittivity ε' and losses tan δ of one of our samples are plotted in Fig. 3 as thick (heating) and thin (cooling) lines, together with the compliance s' and elastic losses Q^{-1} as closed (heating) and open (cooling) symbols. In spite of the limited maximum temperature, it is possible to see a step in the ε' curves that correlates very well with the peak in s'. These compliance curves s' and particularly the acoustic losses are sharply peaked at a temperature T_2 with only 13 K of hysteresis between heating and cooling and allow us to define a precise temperature for the R-T transition (note the sharpness of the losses at higher frequency at T_2 in Fig. 1). In the light of the most recent experiments,[1,13,16] the temperature T_2 can be identified with the onset of the appearance of the R structure, which however appears gradually as a modulation between the M-type in-phase tilts of the octahedra about the c axis in the T phase and the R-type antiphase tilts of the R phase,[13] or as finely twinned R phase.[16] Again, the fact that the anomaly is sharp and pronounced in the elastic compliance and less defined in the dielectric susceptibility suggests that the primary order parameter is the R-type tilting of the octahedra, which in turn induces a change in the direction and amplitude of the cation shifts. Conversely, there is no trace of the ferroelectric transition at T_d in the elastic compliance. This may also be due to the fact that the ferroelectric transition does not seem to involve a change in the structure, but only in the size and correlation length of the domains.

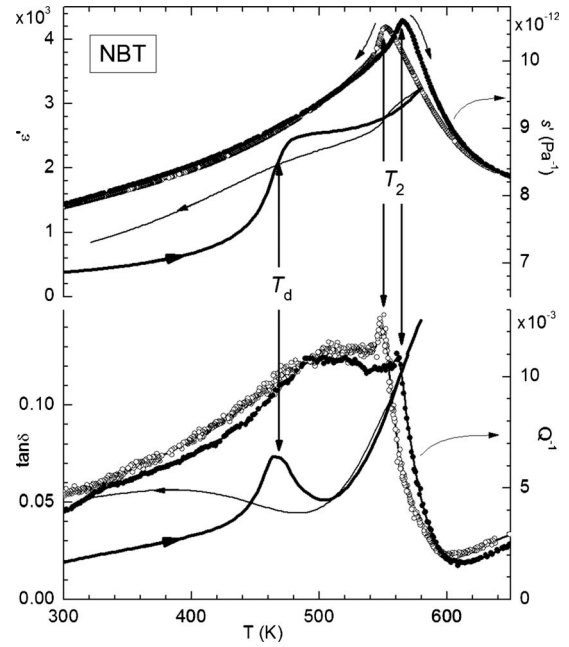The present measurements do not allow yet to unify the different pictures of the R phase obtained from various techniques into a coherent one, but indicate that, in spite of the various indications of extreme heterogeneity on the local scale, short correlation lengths and relaxorlike behavior, the R-type instability responsible for the R phase produces an elastic anomaly comparable to those of other crystalline perovskites with normal structural transitions occurring at a well defined temperature.

The above data can be compared with $c_{11}(T)$ measured on a NBT crystal with the ultrasonic pulse echo technique,[6] where a shallow minimum is found near 580 K, with $\sim$25 K of hysteresis between heating and cooling. The minimum has been attributed to relaxation of the polar regions rather that to the phase transition itself, and, although its temperature is close to T_2, it is much shallower than the peak in the reciprocal Young's modulus $s'(T)$. Considering that the phase transition at T_2 involves the rhombohedral distortion, it is possible that the sharper response of the Young's modulus is mainly due to the shear elastic constants of c_{44} symmetry. Two Brillouin scattering experiments, which probe the acoustic properties at much higher frequencies, yield still different results. In one case[5] a dip in sound velocity and a peak in damping are found near 700 K, which, instead of coinciding with one of the temperatures of the T-C and R-T transitions, is between the two. The observation has been explained in terms of strong fluctuations of the two coupled order parameters for the two T and R phases, plus disorder in the Na/Bi sublattice and has been put in parallel to relaxor ferroelectrics. In a more recent experiment,[4] the intensity of the quasielastic light scattering and a distortion of the phonon peaks from a Lorentzian shape are found to be peaked at 550 K, which is about T_2.
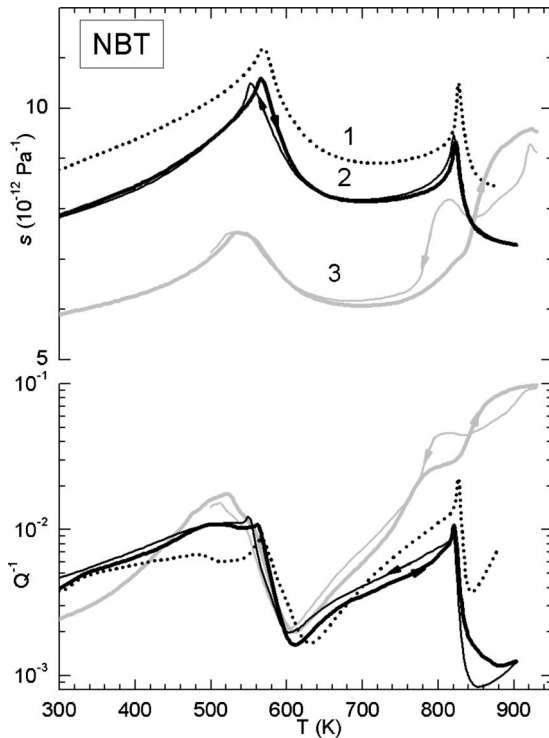

FIG. 3. Left ordinates, continuous lines: dielectric permittivity ε' and losses tan δ of NBT measured at 1 kHz on heating (thick) and cooling (thin). Right ordinates, circles: elastic compliance s' and energy loss Q^{-1} of NBT measured at 1.5 kHz on heating (closed) and cooling (open).

FIG. 4. Reciprocal Young's modulus s' and elastic energy loss Q^{-1} measured on heating (thick lines) and cooling (thin lines) at $\sim$1.4 kHz on three samples of NBT prepared as described in the text.

B. Samples quality

It is true that different techniques may produce different pictures of a same system; for example local probes like the NMR or EXAFS spectroscopies indicate larger and more disordered cation displacements than diffraction techniques.[27] Yet, the quality of samples is important for NBT, since different samples may give different results from the same technique, notably in the dielectric and ferroelectric properties. The main issues are cation ordering, stoichiometry and related defects providing ionized electronic charges. Regarding cation ordering, there are ferroelectric perovskites like $Pb(Sc_{0.5}Ta_{0.5})O_3$ (PST), where the level of Sc/Ta ordering can be controlled and produces marked effects on the temperature and diffuseness of the ferroelectric transition.[28] In NBT, in some case superlattice $\frac{a}{2}(111)$ peaks have been observed by x-ray diffraction[29] or TEM (Refs. [30] and [31]) and attributed to an alternation of Bi and Na along the three directions, but usually cation order is found to be very weak and localized[32] or absent,[2] so that a random distribution is assumed.[14] The level of cation ordering in NBT and its solid solutions with other perovskites is not controllable as in PST, and prolonged annealings in order to improve ordering might rather cause loss of Bi,[33] so that a spread of the NBT properties from sample to sample is not surprising. It is therefore appropriate to check whether the sharp elastic anomalies of NBT in Fig. 1 are the result of a sample of exceptional quality.

Figure 4 shows the anelastic spectra of three samples of NBT prepared in different ways. Samples 1 and 2 were cal-

cined for 1 h at 800 °C (sample 1) or 700 °C (sample 2) and sintered for 2 h at 1150 °C with surrounding NBT packs in order to avoid Bi loss, while sample 3 was prepared with the same temperature schedules of sample 1 but without precautions against Bi loss. Sample 2 is the one of Fig. 1.

It is apparent that the Bi/Na stoichiometry is an issue, since in sample 3 only a reminiscence of the T-C transition at T_1 remains with the sign of the step in the compliance even reversed, and also the transition at T_2 is smeared; in addition, strong irreversible relaxation phenomena occur above 750 K, which are absent in the stoichiometric samples. Such relaxation processes appear as an elastic energy loss two orders of magnitude larger than in the cubic phase of stoichiometric samples, and are presumably due to the migration of the light Na ion by a vacancy mechanism in the cation deficient Na/Bi sublattice. The effect is absent in a perfectly stoichiometric lattice. The dielectric susceptibilities of two samples prepared as sample 1 and 3 (not shown here) demonstrate that the less stoichiometric samples of type 3 are indeed of extremely bad quality also from the dielectric point of view, with enormous losses due to mobile charges, which totally conceal the transition at T_d. On the other hand, samples of type 1 present $\varepsilon(T)$ curves entirely comparable to those of "good" samples in the literature; therefore, the sharp elastic anomalies at T_2 should not be ascribed to an exceptional quality of those samples, but are a general property of NBT. In addition, the elastic anomaly at T_2 clearly persists, although broadened, also in less stoichiometric samples of type 3, where the other transitions are washed out. This demonstrates that the rotational instability leading to the R-T transformation is also robust against lattice disorder.

C. Anelastic spectra of NBT-BT

Figure 5 presents compliance s' and elastic energy losses Q^{-1} curves measured on heating of a series of samples with Ba substitution up to 6%. We do not include the curves for 8% for clarity and because we consider those measurements preliminary, due to the sample quality.

Upon substitution of Ba, the T-C transition lowers its temperature T_1 (continuous arrows), broadens and fades away, until at $x=0.06$ it is no more discernible from the broad maximum that develops around $T_{me} \sim 450$ K. The R-T transition also lowers its temperature T_2 (dashed arrows), and the corresponding elastic anomaly looses intensity and sharpness, but remains always clearly visible. The peak in both the real and imaginary parts of the compliance maintains a rather sharp component at a decreasing T_2, but its weight decreases in favor of a broad maximum at T_{me} which is predominant already at $x=0.03$. The existence of two distinct anomalies at T_2 and T_{me} can be related to fact that there are at least three interacting but distinct order parameters, namely M-type and R-type rotations and cation shifts. Accordingly, the compliance presents three main anomalies: the one at T_1 is obviously related to the M rotations responsible for the tetragonal distortion, while the other two should involve R-type rotations and cation displacements. The identification of the step with the R/T transition, and therefore the R-type rotations, is clear at $x=0$ and $x=0.06$, where the temperature T_2 so de-
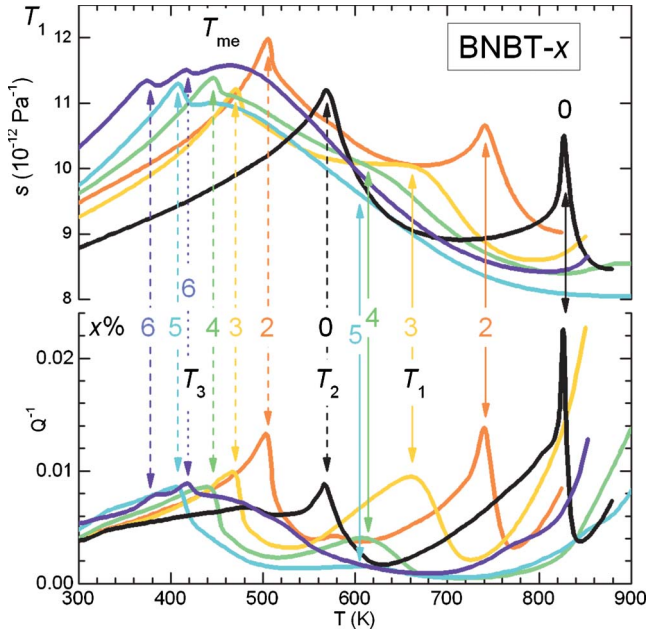
FIG. 5. (Color online) Reciprocal Young's modulus s' and elastic energy loss Q^{-1} of a series of $(NBT)_{1-x}(BT)_x$ samples with $0 \leq x \leq 0.06$ measured at ~ 1.4 kHz. The solid arrows indicate T_1, the dashed arrows T_2 and the dotted T_3.

fined coincides with that determined for the R/T transition by other techniques, and should therefore hold also for the intermediate temperatures (see also the phase diagram below). We remain with the cation shifts as the main responsible for the maximum at T_{me}.

Anomaly at T_3

At $x=0.06$ a new anomaly appears at a temperature indicated as T_3 (dotted arrow) in Fig. 5. It would be natural to identify it with the ferroelectric transition at T_d, but two observations cast doubts on this assignment. One is that T_d deduced from the kink in ε' and from the separation of the dielectric curves measured during heating and cooling is slightly different from T_3. Figure 6 compares the anelastic and dielectric curves of two samples of BNBT-6, where the correlation between the anomalies at T_2 is excellent (hardly visible in ε' but clear in tan δ) but the identification of T_3 with T_d is dubious. The other observation is that in the elastic compliance of NBT there is no trace of T_d (see Fig. 1) and one would expect the same behavior at $x=0.06$, unless the ferroelectric transition has changed nature. Indeed, at $x=0$ the temperature T_d separates a FE-R from a AFE-R phase, while at $x=0.06$ it separates the FE-T phase from a presumably AFE-C or pseudocubic one. Notice that the anomalies of both permittivity and compliance are evident during heating but disappear during cooling, indicating that in the highly disordered NBT-BT there is a slow structural evolution in the R phase, presumably domain coarsening. This is confirmed by the fact that the anomalies on heating require few days of aging at room temperature in order to fully develop. The dashed anelastic curves in Fig. 6 are the result of one week of aging at room temperature after a measurement at high
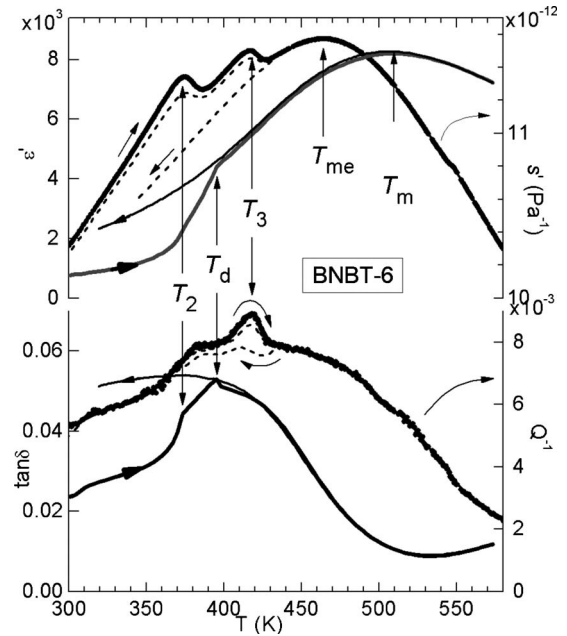

FIG. 6. Left ordinates, continuous lines: dielectric permittivity ε' and losses tan δ of a sample of $(NBT)_{1-x}(BT)_x$ with $x=0.06$ measured at 1 kHz on heating (thick) and cooling (thin). Right ordinates, circles: elastic compliance s' and energy loss Q^{-1} measured at 1.4 kHz on heating; dashed lines: repetition of the measurement (heating and subsequent cooling) after one week of aging at room temperature.

temperature, and the two elastic anomalies are not yet fully developed.

D. Dielectric spectra

The dielectric spectra have been extensively discussed,[34–39] and here we point out only the main conclusions and some differences with respect to the previous literature. In Fig. 7 a panoramic of the dielectric permittivity and losses measured at 10 kHz during heating of $(NBT)_{1-x}(BT)_x$ with $0 \leq x \leq 0.08$ is shown. The samples with 2% and 3% Ba had rather high conductivities and hence losses, but the real part ε' at 10 kHz, where the influence of such conductivity effects is reduced, fit well the general trend of growing maximum of ε' at T_m and lowering T_d with increasing x. The step at T_2 is invisible in this scale at $x=0$ (but see Fig. 3), it is indistinguishable from the ferroelectric transition due to the coincidence of T_2 and T_d for $x \geq 0.02$ but it is again separated from T_d at $x=0.06$. A first difference between our measurements and those of Hiruma *et al.*[34] is that we see a single dielectric anomaly already at $x=0.02$ while they observe such a merging at $x=0.03$. We also observed that temperature and width of these steps depend on the sample preparation and the polarization status, being generally sharper and at higher temperature in poled samples.

Regarding the frequency dispersion of the dielectric maximum and the presence of a secondary maximum with even stronger frequency dispersion near T_d,[35,36] Fig. 8 shows the dielectric permittivity of an initially poled sample with $x=0.04$ measured at different frequencies. There is some fre-
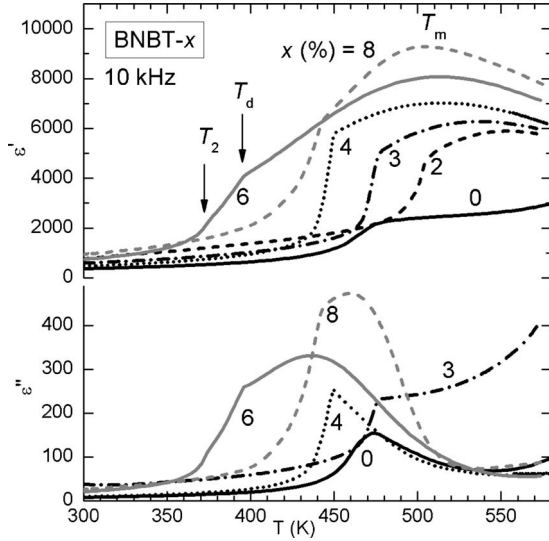
FIG. 7. Real and imaginary parts of the dielectric permittivity of a series of samples with $0 \leq x \leq 0.08$ measured during heating at 10 kHz.

FIG. 9. (Color online) Phase diagram of $(NBT)_{1-x}(BT)_x$ deduced from the present anelastic and dielectric (10 kHz) measurements. Grey lines: T_m, T_2, T_d from Ref. 34. C=cubic, T=tetragonal, R=rhombohedral, F=ferroelectric, $\sim$A=almost antiferroelectric, P=paraelectric.

quency dispersion at $x \geq 0.04$, although of reduced magnitude with respect to what found in typical relaxor ferroelectrics, but we never found the secondary maximum near T_d; we only find a neat step during heating in the poled state, with reduced sharpness and temperature during cooling, or heating in the unpoled state. The secondary maximum has been associated with an incommensurate modulation between FE and AFE state,[38,39] as found in the highly ordered ferroelectric perovskite $Pb(Yb_{0.5}Ta_{0.5})O_3$.[40] Incommensurate modulation of the R phase along the c axis of the parent T phase has indeed been found by neutron diffraction[13] and its persistence after the disappearance of the T phase has been suggested to be due to some type of ordering in the Na/Bi
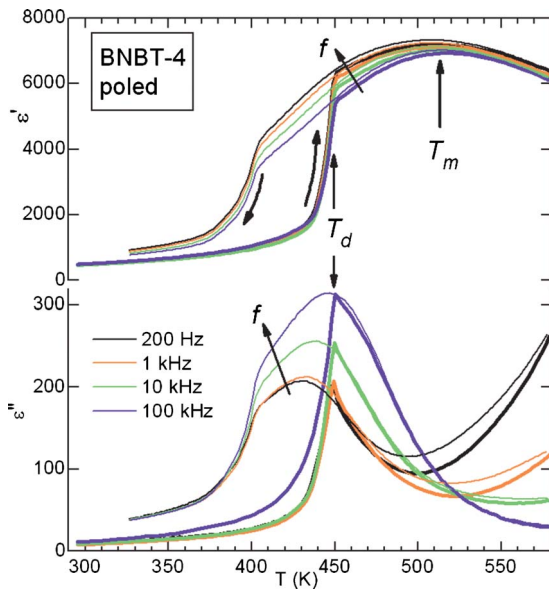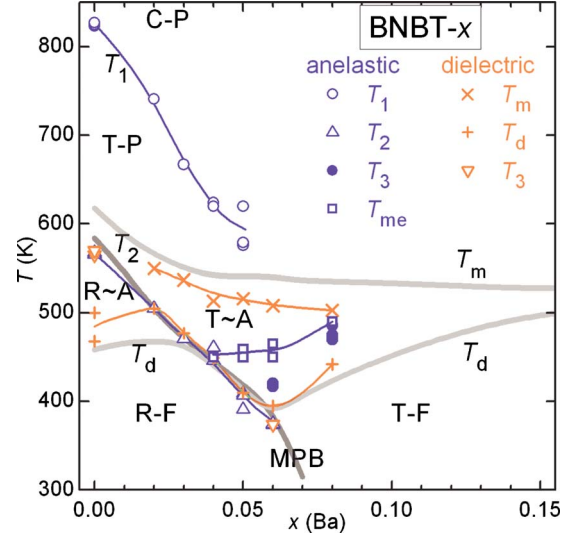
sublattice. Also TEM experiments indicate a R phase modulated by twins,[1,16] but at $T > T_d$.

Our dielectric and anelastic spectra do not show features necessarily ascribable to incommensurate modulations; the anelastic losses remain high also below T_2 and T_d, but this might also be due to generic domain wall motion. Apparently, such walls may give rise to incommensurate modulations, whose morphology likely depends on the sample quality. In this respect, we recall that the dielectric hump that is presumed to accompany incommensurate modulations is enhanced by introducing cation vacancies through La doping[41] or in solid solution with $K_{0.5}Bi_{0.5}TiO_3$ (Ref. 42–44) or $BaTiO_3$.[37] It is therefore likely that the exact stoichiometry and degree of ordering of cations determine the detailed structural distortions, their correlation lengths and domain morphologies, and the scarce consistency between the results of various experiments is not only due to differences in the properties that are probed but also in the quality of the samples.

E. Phase diagram

Figure 9 shows the phase diagram of $(NBT)_{1-x}(BT)_x$ deduced from the present anelastic and dielectric (10 kHz) measurements during heating, together with that available in the literature[34] (gray lines T_m, T_2, T_d). The latter is mainly based on dielectric measurements and therefore does not include the border between T and C phases. It is sometimes assumed that the paraelectric phase above T_m is cubic, but this cannot be the case at low enough x, since the neutron diffraction data show that NBT is tetragonal above T_m and becomes cubic only at $T_1 = 820$ K.

The anelastic spectra of Fig. 5 allow us to draw a $T_1(x)$ line that drops rapidly toward T_m, roughly at the composition of the MPB; similarly to the NBT-PbTiO$_3$ phase diagram.[45]

FIG. 8. (Color online) Real and imaginary parts of the permittivity ε of an initially poled sample of $(NBT)_{1-x}(BT)_x$ with $x = 0.04$.

It is not clear whether T_1 merges with the $T_m(x)$ line at $x > 0.05$ or dissolves into an average cubic phase with local tetragonal distortions. The three open circles at $x = 0.05$ refer to three different samples where the anomaly at T_1 is extremely shallow and broadened. The region of the phase diagram defined by $x > 0.05$ and $T_d < T < T_m$ is of uncertain nature. In $(NBT)_{1-x}(BT)_x$ codoped with Zr, with a particularly evident relaxorlike frequency dispersion in ε' near T_d, such a region has been defined as a frustrated region with coexistence of "multiple domain states.[46]" The fading away of the anelastic anomaly at T_1 with increasing x suggests that for $x > 0.05$ and $T > T_d$ the phase is pseudocubic with local tetragonal distortions whose correlation length must be very small.

The temperature T_m of the broad maximum of $\varepsilon'(T)$ is somewhat lower than in Ref. 34, while the temperature T_{me} of the maximum of the compliance is up to 60 K lower than T_m. A similar phenomenon occurs in the relaxor ferroelectrics $Pb(Mg_{1/3}Nb_{2/3})_{1-x}Ti_xO_3$ and $(Pb/La)(Zr/Ti)O_3$, where the dielectric maximum is at a temperature higher than the maximum of the elastic compliance but also of the susceptibility deduced from NMR relaxation[47,48] (but, unlike dielectric and anelastic spectroscopies, NMR probes also excitations with $q > 0$, see Ref. 49). This has been explained as the result of the different sensitivity of the three techniques to the polar on one hand and nonpolar rotational degrees of freedom on the other hand, all exhibiting a relaxational dynamics which is faster for the rotational ones.[48] Indeed, also the dielectric maximum in NBT-BT acquires a dispersion in frequency with Ba doping. In NBT-BT, however, the R-type rotational degrees of freedom undergo a phase transformation at T_2; therefore, the elastic maximum at T_{me} should involve other rotational degrees of freedom, possibly also M-type rotations, which are coupled to the polar modes and hence yield dielectric and elastic susceptibility maxima at similar temperatures.

The $T_2(x)$ line separating the R from the T phases joins $T_d(x)$ very soon, at $x = 0.03$ according to Hiruma *et al.*[34] and already at $x = 0.02$ after our measurements. There is some variability in the values of T_2 determined from the dielectric curves, depending on the polarization state, but overall there is good agreement with T_2 determined from the anelastic spectra on unpoled samples. At $x \geq 0.06$ the $T_d(x)$ line starts rising, while $T_2(x)$ continues to decrease, determining the MPB.

As noted in the previous paragraphs, the dielectric anomaly at T_2 may be not very sharp, especially in unpoled samples, and the marked anomalies measured at $0.02 \leq x \leq 0.06$ may mainly reflect the ferroelectric transition. The compliance, however, is almost unaffected by the ferroelectric transition, and always presents a sharp step at T_2. This means that the rotational instability of R type has a clear onset at a well defined temperature T_2 also at compositions where $(NBT)_{1-x}(BT)_x$ displays properties typical of highly disordered or relaxor systems. Notably, the sharp step in s' coexist with the broad maximum at T_{me} and a T-C transition that is almost completely faded away at $x \geq 0.05$ (see Figs. 5 and 6). It turns out, therefore, that the polar modes are strongly affected by disorder, characterized by short correlation lengths and undergo a diffuse or relaxor transition; on

the other hand, the R-type modes undergo a phase transition which is well behaved from the elastic point of view, presumably with a long correlation length.

F. Morphotropic phase boundary and possible monoclinic phase

The composition-temperature phase diagrams of various solid solutions between a perovskite which is rhombohedral at low temperature and one which is tetrahedral, have an almost vertical line that separates the two phases and is called morphotropic phase boundary (MPB). Among the most studied ferroelectric systems of this type are PZT (Ref. 50) and PMN- PT.[51] After decades of studies on PZT, it has been found that an intermediate monoclinic phase exists in a narrow region at the MPB.[52] The identification of such a monoclinic phase, where the direction of the polarization may continuously vary between those in the R and T phases, was possible from high-resolution synchrotron x-ray diffraction experiments and careful analysis of the neutron diffraction data. The possibility for the polarization to continuously rotate between the T and R phases through the monoclinic one is still debated,[53,54] but is generally considered as the key factor that yields an easy change of polarization under stress and therefore high electromechanical coupling at the MPB compositions.[55]

The solid solution NBT-BT at room temperature passes from R to T at the composition $x \sim 0.06$, which is generally identified with the MPB, and where the electromechanical coupling is maximum. Actually, there are few studies aimed at defining the MPB line $T_2(x)$,[34,56] which is defined by only two points at $x = 0.06$ and 0.07. Other tetragonal perovskites that give rise to a MPB with NBT are $PbTiO_3$ (Ref. 45) and $K_{0.5}Bi_{0.5}TiO_3$, but in the latter the composition of KBT at the border between R and T at room temperature has been reported to range between 0.17 and 0.8.[44]

Besides better defining the MPB line, it would be interesting to investigate whether also NBT-BT has an intermediate monoclinic phase that allows continuous rotation of the polarization between the pseudocubic [100] and [111] directions. The identification of a monoclinic phase by diffraction would certainly be more difficult for $(NBT)_{1-x}(BT)_x$ than for PZT, due to the larger disorder caused by the coexistence of ions with different charges, Na^+, Bi^{3+}, and Ba^{2+} in the A sublattice with respect to Zr^{4+} and Ti^{4+}, which have the same charge. The signature of the M phase should be more evident in the elastic compliance versus temperature: in fact, the reciprocal Young's modulus of PZT has a large peak in correspondence with the MPB,[57] that may be simply explained in terms of the usual Landau free energy expansion with a coupling term linear in strain and quadratic in the polarization, if the polarization may rotate in a monoclinic phase instead of switching between R and T phases.[57]

The case of $(NBT)_{1-x}(BT)_x$ is more complicated than PZT, since there is no single transformation between T and M, but two distinct processes: a R-T transformation at T_2 and a diffuse transformation around T_{me} and T_m. The first is well behaved from the elastic point of view, with the expected sharp step in the compliance at the R-type rotational

instability.[24] If monoclinic distortions exist, they must be connected with the diffuse process. The fact that it is the main feature in the dielectric susceptibility indicates that it is due to polar modes, while the strong peaked response in the elastic compliance recalls the behavior of the monoclinic phase of PZT. At variance with PZT, however, there should not be a monoclinic phase, but only local monoclinic distortions with short correlation lengths, thereby producing a diffuse response. This is in agreement with recent NMR (Ref. 27) and diffuse x-ray scattering experiments,[18] both revealing additional displacements of the Na/Bi ions away from the rhombohedral $\langle 111 \rangle$ direction along $\langle 100 \rangle$, producing a local monoclinic symmetry. The existence of monoclinic regions is also supported by a diffuse scattering experiment,[18] from which it can be deduced that they are shaped as platelets one or two cell thick and 20 nm wide.

IV. CONCLUSIONS

We measured the complex dielectric permittivity and elastic compliance of $(NBT)_{1-x}(BT)_x$ with $0 \leq x \leq 0.08$. The anelastic spectra contain anomalies at both the temperatures T_1 and T_2 of the tetragonal-cubic and tetragonal-rhombohedral transitions, plus a broad maximum at a temperature T_{me}, which is up to 60 K lower then T_m of the diffuse dielectric maximum. The $T_1(x)$ line in the $x-T$ phase diagram drops rapidly with x and can be followed up to $x \simeq 0.05$, where the transition becomes so diffuse and weak to be hardly recognizable. At higher Ba substitution, the high temperature structure should be pseudocubic with short range tetragonal distortions. Instead, the elastic anomaly at T_2 is extremely sharp in pure NBT and remains distinct up to $x=0.06$, demonstrating that there is a well defined onset of the R-type octahedral rotations producing the R structure, in spite of the numerous indications of extremely diffuse transition and structural heterogeneity. The dielectric permittivity in our samples does not have a secondary maximum with frequency dispersion around the ferroelectric transition at T_d, as often reported; instead, we observe steps both at T_d and T_2 (which

however coincide for $0.02 \leq x \leq 0.05$), whose exact temperature and sharpness depend on the sample state and polarization. These features are common to samples prepared under different temperature and time schedules, if precautions are taken in order to avoid Bi loss during sintering; otherwise, the anelastic and dielectric spectra indicate extremely blurred structural transformations and defective material, especially above 800 K, where Na diffusion becomes possible through the vacancy mechanism.

The anelastic and dielectric anomalies should be connected to the nonpolar rotational modes of the octahedra and polar cation displacement as follows. The M-type rotations giving rise to the T phase becomes unstable at T_1, but the correlation length of such modes rapidly decreases with Ba substitution, so that at $x > 0.05$ no long range T order exists any more. The R-type rotations giving rise to the R distortion are unstable at T_2, and maintain long range correlations up to $x=0.06$, which is the Ba composition of the morphotropic phase boundary. The diffuse dielectric maximum at T_m and elastic maximum at T_{me} should be due to polar modes, whose correlation length remains short unless an external poling field is applied or aging of the order of several days at room temperature is allowed.

With Ba substitution, the broad peak in the elastic compliance becomes preponderant over the R-T transition and, by analogy with the behavior of PZT with monoclinic structure at the MPB, the possibility is discussed that on the local scale the polarization may have an intermediate direction between R and T.

[1] V. Dorcet, G. Trolliard, and P. Boullay, Chem. Mater. **20**, 5061 (2008).

[2] G. O. Jones and P. A. Thomas, Acta Crystallogr., Sect. B: Struct. Sci. **58**, 168 (2002).

[3] I. P. Aleksandrova, A. A. Sukhovsky, Yu. N. Ivanov, Yu. E. Yablonskaya, and S. B. Vakhrushev, Ferroelectrics **378**, 16 (2009).

[4] A. I. Fedoseev, S. G. Lushnikov, S. N. Gvasaliya, P. P. Syrnikov, and S. Kojima, Phys. Solid State **51**, 1399 (2009).

[5] I. G. Siny, C.-S. Tu, and V. H. Schmidt, Phys. Rev. B **51**, 5659 (1995).

[6] J. Suchanicz, J. Mater. Sci. **37**, 489 (2002).

[7] A. S. Nowick and B. S. Berry, *Anelastic Relaxation in Crystalline Solids* (Academic Press, New York, 1972).

[8] C.-S. Tu, I. G. Siny, and V. H. Schmidt, Phys. Rev. B **49**, 11550 (1994).

[9] T. Oh and M.-H. Kim, Mater. Sci. Eng., B **132**, 239 (2006).

[10] Y. Hiruma, H. Nagata, and T. Takenaka, J. Appl. Phys. **104**, 124106 (2008).

[11] S. B. Vakhrushev, V. A. Isupov, B. E. Kvyatkovsky, N. M. Okuneva, I. P. Pronin, G. A. Smolensky, and P. P. Syrnikov, Ferroelectrics **63**, 153 (1985).

[12] J. Suchanicz, Mater. Sci. Eng., B **55**, 114 (1998).

[13] A. M. Balagurov, E. Yu. Koroleva, A. A. Naberezhnov, V. P. Sakhnenko, B. N. Savenko, N. V. Ter-Oganessian, and S. B. Vakhrushev, Phase Transitions **79**, 163 (2006).

[14] J. Petzelt, S. Kamba, J. Fábry, D. Noujni, V. Porokhonskyy, A. Pashkin, I. Franke, K. Roleder, J. Suchanicz, R. Klein, and G. E. Kugel, J. Phys.: Condens. Matter **16**, 2719 (2004).

[15] I. P. Aleksandrova, Yu. N. Ivanov, A. A. Sukhovskii, and S. B.

Vakhrushev, Phys. Solid State **48**, 1120 (2006).

[16] V. Dorcet, G. Trolliard, and P. Boullay, J. Magn. Magn. Mater. **321**, 1758 (2009).

[17] S. G. Lushnikov, S. N. Gvasaliya, I. G. Siny, I. L. Sashin, V. H. Schmidt, and Y. Uesu, Solid State Commun. **116**, 41 (2000).

[18] J. Kreisel, P. Bouvier, B. Dkhil, P. A. Thomas, A. M. Glazer, T. R. Welberry, B. Chaabane, and M. Mezouar, Phys. Rev. B **68**, 014113 (2003).

[19] J. Hlinka, J. Petzelt, S. Kamba, D. Noujni, and T. Ostapchuk, Phase Transitions **79**, 41 (2006).

[20] H. Y. Tian, D. Y. Wang, D. M. Lin, J. T. Zeng, K. W. Kwok, and H. L. W. Chan, Solid State Commun. **142**, 10 (2007).

[21] Y. Hiruma, H. Nagata, and T. Takenaka, Jpn. J. Appl. Phys. **45**, 7409 (2006).

[22] A. M. Glazer, Acta Crystallogr., Sect. B: Struct. Sci. **28**, 3384 (1972).

[23] U. J. Nicholls and R. A. Cowley, J. Phys. C **20**, 3417 (1987).

[24] M. A. Carpenter and E. H. K. Salje, Eur. J. Mineral. **10**, 693 (1998).

[25] J. Suchanicz, J. Phys. Chem. Solids **62**, 1271 (2001).

[26] Y. Qu, D. Shan, and J. Song, Mater. Sci. Eng., A **121**, 148 (2005).

[27] I. P. Aleksandrova, A. A. Sukhovsky, Yu. N. Ivanov, Yu. E. Yablonskaya, and S. B. Vakhrushev, Phys. Solid State **50**, 496 (2008).

[28] N. Setter and L. E. Cross, J. Appl. Phys. **51**, 4356 (1980).

[29] S.-E. Park, S.-J. Chung, I.-T. Kim, and K. S. Hong, J. Am. Ceram. Soc. **77**, 2641 (1994).

[30] J.-K. Lee, J. Y. Yi, and K.-S. Hong, Jpn. J. Appl. Phys. **40**, 6003 (2001).

[31] J.-K. Lee, K. S. Hong, C. K. Kim, and S.-E. Park, J. Appl. Phys. **91**, 4538 (2002).

[32] D. I. Woodward and I. M. Reaney, Acta Crystallogr., Sect. B: Struct. Sci. **61**, 387 (2005).

[33] Y. Hiruma, H. Nagata, and T. Takenaka, J. Appl. Phys. **105**, 084112 (2009).

[34] Y. Hiruma, Y. Watanabe, H. Nagata, and T. Takenaka, Key Eng. Mater. **350**, 93 (2007).

[35] V. A. Isupov, Ferroelectrics **315**, 123 (2005).

[36] S. Said and J.-P. Mercurio, J. Eur. Ceram. Soc. **21**, 1333 (2001).

[37] J.-R. Gomah-Pettry, S. Saïd, P. Marchet, and J.-P. Mercurio, J. Eur. Ceram. Soc. **24**, 1165 (2004).

[38] J.-K. Lee, J. Y. Yi, and K. S. Hong, J. Appl. Phys. **96**, 1174 (2004).

[39] C. Zhou, X. Liu, W. Li, C. Yuan, and G. Chen, J. Mater. Sci. **44**, 3833 (2009).

[40] N. Yasuda and J. Konda, Appl. Phys. Lett. **62**, 535 (1993).

[41] J. Y. Yi, J.-K. Lee, and K. S. Hong, Ferroelectrics **270**, 203 (2002).

[42] J. Suchanicz, J. P. Mercurio, K. Konieczny, and T. V. Kruzina, Ferroelectrics **290**, 161 (2003).

[43] X. Yi, H. Chen, W. Cao, M. Zhao, D. Yang, G. Ma, C. Yang, and J. Han, J. Cryst. Growth **281**, 364 (2005).

[44] H. Xie, L. Jin, D. Shen, X. Wang, and G. Shen, J. Cryst. Growth **311**, 3626 (2009).

[45] K. S. Hong and S.-E. Park, J. Appl. Phys. **79**, 388 (1996).

[46] S. A. Sheets, A. N. Soukhojak, N. Ohashi, and Y.-M. Chiang, J. Appl. Phys. **90**, 5287 (2001).

[47] F. Cordero, F. Craciun, and P. Verardi, Ferroelectrics **290**, 141 (2003).

[48] F. Cordero, M. Corti, F. Craciun, C. Galassi, D. Piazza, and F. Tabak, Phys. Rev. B **71**, 094112 (2005).

[49] B. E. Vugmeister, Phys. Rev. B **73**, 174117 (2006).

[50] B. Noheda and D. E. Cox, Phase Transitions **79**, 5 (2006).

[51] M. Davis, J. Electroceram. **19**, 25 (2007).

[52] R. Guo, L. E. Cross, S.-E. Park, B. Noheda, D. E. Cox, and G. Shirane, Phys. Rev. Lett. **84**, 5423 (2000).

[53] J. Frantti, Y. Fujioka, and R. M. Nieminen, J. Phys.: Condens. Matter **20**, 472203 (2008).

[54] E. P. Smirnova, A. V. Sotnikov, O. E. Kvyatkovskii, M. Weihnacht, and V. V. Lemanov, J. Appl. Phys. **101**, 084117 (2007).

[55] H. Fu and R. E. Cohen, Nature (London) **403**, 281 (2000).

[56] T. Takenaka, K. Maruyama, and K. Sakata, Jpn. J. Appl. Phys., Part 1 **30**, 2236 (1991).

[57] F. Cordero, F. Craciun, and C. Galassi, Phys. Rev. Lett. **98**, 255701 (2007).